

## MORPHOLOGICAL CHARACTERISTICS OF NONLINEAR OPTICAL MOLECULES AT THE AIR/WATER INTERFACE

SUNG-TAEK LIM<sup>1</sup>, MI-KYUNG PARK<sup>1</sup>, OHOAK KWON<sup>2</sup> and DONG-MYUNG SHIN<sup>1\*</sup>

<sup>1</sup>Department of Chemical Engineering, Hong-Ik University, Seoul 121-791, Korea

<sup>2</sup>Korea Basic Science Center, Seoul Branch, Seoul 136-701, Korea

(Received 28 April 1997; accepted 18 March 1998)

**Abstract** – The texture change of non-linear optical molecules at the air/water interface was investigated as a function of surface pressure with Brewster angle microscopy. The texture change resulted from the aggregation of dye molecules is important to understand the film uniformity and grain formation process. The 4-Octadecylhydroxy-4'-nitrostilbene (OHNS) generated the small spots of size around 1  $\mu\text{m}$ . The spots exhibit high contrast with other film area and do not show angle dependent reflectivity change. It is interesting to observe that the size of the domain stays the same as the film pressure increases. At high surface pressure, the contrast ratio of domains becomes high, which means dense packing of OHNS. And, the size of domain grows. In the middle of domain, highly contrasted domains are formed. The first and the second order transitions of OHNS observed from surface pressure-area isotherm result from the two types of grains. The N,N-Dihexadecylcyanoaniline (DHCA) formed highly contrasted grains over entire region, and the grains are the double layers. The difference in Langmuir film of OHNS and DHCA at the air/water interface is consistent with the small tilt angle from the surface normal for OHNS and the large tilt angle for DHCA in the Langmuir-Blodgett films.

### INTRODUCTION

Brewster angle microscopy (BAM) is an important technique for the understanding of phase transitions, texture and polarization of thin films at air-water interfaces.<sup>1-7</sup> The method is based on measurement of the change in the state of polarization when electromagnetic wave reflected from thin films which locate in between two isotropic media. Such changes depend on the thickness of the films and its anisotropy. If the polarized incident beam strikes the interface at the Brewster angle of the bare surface, essentially all the background related to the substrate is eliminated and the method is sufficiently sensitive to allow images of monolayers at the air/water interface. Optical anisotropy can be obtained from the ratio of p- and s- polarized light. However, the ratio of reflected p- and s-polarized light is very small at the Brewster angle, which, together with the polarizer used for the incident light, provides that an extinction ratio is very much higher than that could be obtained with a single polarizer in ordinary polarized microscopy.

There are several studies by BAM in which phase boundaries have been determined by observations of qualitative changes in monolayer textures. Isotropic phases can be distinguished by the difference in their

thickness. The transitions between a phase in which the molecules are tilted to one in which the molecules are normal to the surface or transitions between phases in which there are differences in the molecular tilt order can be detected by changes in anisotropy.

The textures of monolayer are surprisingly complex. There is often large-scale organization of the molecular tilt azimuth into regular arrays of stripes, spirals, and stars.<sup>1</sup> These textures are closely related to those observed in liquid crystals, and theories analogous to those developed for liquid crystals are able to describe many of the patterns. Several qualitative comparisons have been made between experimental BAM images of such patterns and images calculated from assumed models of the tilt organization and quantitative analysis of BAM images of tilt order in Langmuir monolayer domains.<sup>1</sup>

We tried to visualize the textures and images of monolayer films that were formed with donor-acceptor aromatic molecules containing long alkyl chain. The films layered at the air/water interface were visualized with BAM. The films experience the first and the second-order phase transition depending upon the barrier speed. Molecules that locate at the air/water interface are favorable to generate syndioregic (head-to-head) orientations.<sup>8</sup> However, overall orientation of the molecules can be obtained with the FT-IR data analysis. We analyzed the FT-IR intensities of CH<sub>2</sub> group and NO<sub>2</sub> group of the donor-acceptor molecules layered as a Langmuir-Blodgett(LB) film. The comparison of BAM

\* To whom correspondence should be addressed.

† Abbreviations: O-octadecyl-4'-nitro-4-hydroxystilbene (OHNS), di-n-hexadecylcyanobenzene (DHCA), arachidic acid (AA), Brewster angle microscopy (BAM), Fourier Transform infrared (FT-IR), Langmuir-Blodgett (LB)

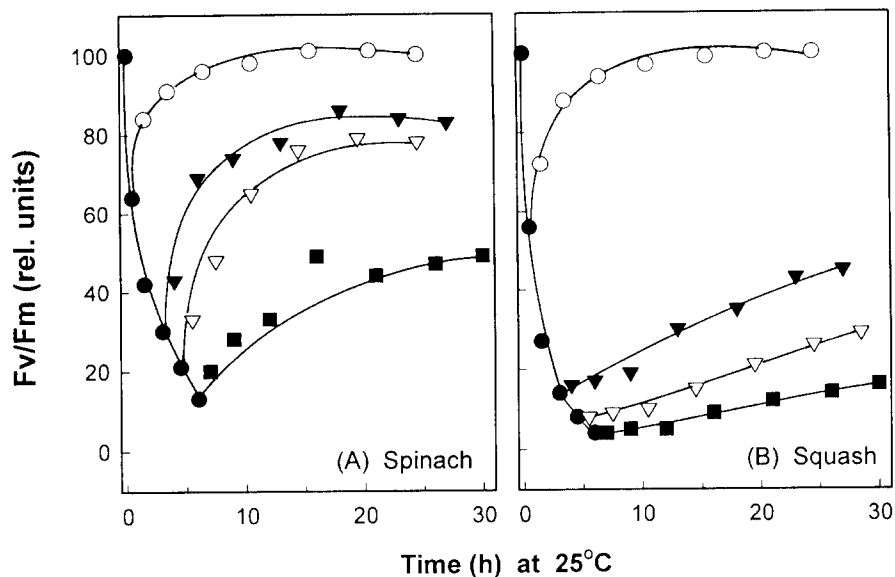


Figure 4. Restoration of Fv/Fm ratios from the photoinhibited state in leaf disks of spinach (A) and squash (B) plants. Leaf disks were exposed to light at an intensity of  $2.8 \text{ mmol m}^{-2} \text{ s}^{-1}$  for different periods at  $25^\circ\text{C}$  to induce photoinhibition. The leaf disks were then incubated at  $25^\circ\text{C}$  in dim light at an intensity of  $0.07 \text{ mmol m}^{-2} \text{ s}^{-1}$  for recovery from photoinhibition. The initial values of Fv/Fm measured at  $25^\circ\text{C}$  was taken as 100% that corresponded to 0.84 and 0.82 in spinach and squash, respectively. The values were obtained from the results of three independent experiments. The deviation of values was  $< 5\%$  in each case. (●) photoinhibitory light treatment; (○) recovery from 0.5h-photoinhibition; (▼) recovery from 3h-photoinhibition; (▽) recovery from 4.5 h-photoinhibition; (■) recovery from 6h-photoinhibition.

photoinhibitory treatment. However, when recovered at  $17^\circ\text{C}$ , spinach showed more rapid recovery of PS II from photoinhibition (Figs. 5C and D), suggesting that recovery of spinach photosynthesis from photoinhibition is not as much dependent on the temperature as that of squash.

Fig. 6 shows temperature-dependent recovery of PS II from photoinhibition in leaves of pea and sweet potato. Leaf disks were exposed to strong light for designated periods of photoinhibition at  $10^\circ\text{C}$  (Figs. 5C and D) and  $25^\circ\text{C}$  (Figs. 5A and B). Then, changes in the ratios of Fv to Fm was monitored in dim light at  $17^\circ\text{C}$  (Figs. 5B and D) and  $25^\circ\text{C}$  (Figs. 5A and C). Pea plants were markedly efficient in recovering PS II from photoinhibition, in contrast to sweet potato plants, which showed severe decline in Fv/Fm after  $10^\circ\text{C}$ -photoinhibition, and showed very minor recovery of PS II even at  $25^\circ\text{C}$

## DISCUSSION

In the present study, we compared the extent of low-temperature photoinhibition in chilling-resistant and chilling-sensitive plants, in relation to the extent of fatty acid unsaturation of thylakoid membrane lipids. When the susceptibility to strong light was compared between spinach and squash, squash was found to be more sensitive to photoinhibition than spinach (Fig. 1) Reductions in PS II photochemical efficiency, measured as the ratio of Fv to Fm (Fv/Fm) do not necessarily

reflect damage to PS II involving, for example, the degradation of thylakoid proteins. These reductions may also indicate a controlled, sustained increase in the thermal dissipation of excess energy occurring, for example, in the antenna chlorophyll, which is closely correlated with a protective role of zeaxanthin.<sup>15</sup>

However, PS II photochemical efficiency is reduced under strong light *via* the photo-induced damage to the reaction center, involving, for example, the breakdown of D1 protein in thylakoid membranes.<sup>16</sup> We attempted to examine this possibility by applying lincomycin, an inhibitor of chloroplast-encoded protein synthesis, to leaves under photoinhibitory treatment. When the leaves were treated with lincomycin before photoinhibitory treatment, the differential susceptibility to strong light, which had been previously observed between the two types of plants, as in Figure 1A-C, became almost indistinguishable, as shown in Figure 1D-F. Based on these observations, we attempted to further examine PS II photoinhibition in terms of light-induced degradation and repair of D1 protein.

Two competing processes are operative, during photoinhibition *in vivo*:<sup>14</sup> light-induced inactivation, which includes damage to the D1 protein of the PS II complex; and the recovery processes, which includes degradation of the damaged D1 protein, synthesis of the D1 protein *de novo* and reintegration of the D1 protein into the PS II complex. To determine which of the two processes is responsible for the difference in sensitivity to photoinhibition between chilling-sensitive and

the sensor unit during recording was digitised by using a fast analog/digital converter. The initial fast rise in the fluorescence signal was digitized to give resolution of the  $F_0$  value, which designates the fluorescence level when all reaction centers of PS II are open - namely when the primary electron acceptors of PS II are fully oxidized. After 2 milliseconds, a slower acquisition rate of data points was adopted (1,000 readings per second) until the recording period is 1 second. Then the key fluorescence parameters of  $F_m$ ,  $F_v$ , and the ratio  $F_v/F_m$  were automatically calculated for the light level used during measurement.  $F_m$  represents the maximal yield of fluorescence emitted from dark-adapted leaves. The variable fluorescence,  $F_v$ , was given by the difference between  $F_m$  and  $F_0$ .<sup>12</sup>

## RESULTS

### Lipids of thylakoid membranes

Lipids were extracted from isolated thylakoid membranes and separated into several lipid classes - namely, monogalactosyl diacylglycerol (MGDG), digalactosyl diacylglycerol (DGDG), sulfoquinovosyl diacylglycerol (SQDG) and PG (Table 1). Except for DGDG, the proportion of the individual lipid classes was not very different between spinach and squash. PG accounted for small proportion - namely, less than 10% of the total polar lipids in the two types of plant, in consistence with the other report.<sup>22</sup>

As shown in Table 2, fatty acid analysis of the isolated thylakoid membrane lipids revealed that spinach plant contained 16:3 in MGDG, a characteristic of 16:3 plants, in contrast to squash plant in which 16:3 is absent in MGDG, a characteristic of 18:3 plants.<sup>13</sup> More importantly, the sum of *cis*-unsaturated fatty acids of PG were 43% and 11% in thylakoid membranes of spinach and squash plants, respectively, indicating that spinach has a higher degree of fatty acid unsaturation in PG than squash by 32% (Table 2). The sum of *cis*-unsaturated fatty acids of PG extracted from leaves of pea and sweet potato was reported to be 42% and 18%, respectively.<sup>6</sup>

### Photoinhibition of photosynthesis in leaves

Table 1. Composition of lipid classes in thylakoid membranes isolated from spinach and squash plants.

Origin of thylakoid membranes	Lipid class, mol %			
	MGDG	DGDG	SQDG	PG
Spinach	64	23	4	8
Squash	59	32	3	6

The values are the means of results from two independent experiments. The deviation of values was < 4% in every case.

Table 2. Fatty acids in polar lipids from thylakoid membranes isolated from spinach and squash plants.

Lipid class	Fatty acid, mol %									$\Sigma$ <i>cis</i> -unsat. FA, mol%
	16:0	16:1c	16:1t	16:3	18:1			18:2	18:3	
					9- <i>cis</i>	11- <i>cis</i>	tr			
Spinach										
MGDG	1	1	tr	19	1	tr	tr	2	74	96
DGDG	9	tr	tr	3	tr	tr	1	3	82	89
SQDG	48	0	2	2	1	0	0	10	37	49
PG	20	0	36	tr	1	tr	1	7	35	43
Squash										
MGDG	2	0	1	0	tr	tr	tr	2	95	97
DGDG	11	0	1	0	1	tr	tr	2	85	87
SQDG	42	0	1	0	3	2	0	4	48	54
PG	69	0	14	0	6	2	1	1	7	11

16:0, Hexadecanoic acid (palmitic acid); 16:1c, 9-*cis*-hexadecenoic acid (palmitoleic acid); 16:1t, 3-*trans*-hexadecenoic acid; 18:0, octadecanoic acid (stearic acid); 18:1, 9-octadecenoic acid (oleic acid) and 11-octadecenoic acid (vaccenic acid); 18:2, 9,12-octadecadienoic acid (linoleic acid); 18:3, 9,12,15-octadecatrienoic acid ( $\alpha$ -linolenic acid); tr, trace (less than 0.5%).  $\Sigma$ *cis*-unsat. FA is the sum of the *cis*-unsaturated fatty acids. The values are the means of results obtained from two independent experiments.

Fig. 1 shows time courses of photoinhibition at 5°C, 15°C and 25°C of the PS II complex in spinach and squash leaves, as determined in terms of ratios of  $F_v$  to  $F_m$ . In the absence of lincomycin (Fig. 1 A-C), the decline in the ratios of  $F_v$  to  $F_m$  was greater at lower temperatures in leaves of both species of plants. However, squash was more susceptible than spinach to photoinhibition at all temperatures tested. The extent of photoinhibition in leaves represents the outcome of the competition between the light-induced inactivation of the PS II complex and the subsequent recovery from the photoinhibited state.<sup>14</sup> In view of this perspective, we separated the two processes into the individual ones by inducing photoinhibition in the presence of lincomycin, an inhibitor of protein synthesis in chloroplasts (Fig. 1 D - F). Lincomycin accelerated photoinhibition in both spinach and squash. Moreover, the difference in the susceptibility to photoinhibition between the two species of plants was indistinguishable in the presence of lincomycin, suggesting that rate of the photo-induced inactivation was about the same in the two species.

### Photoinhibition in isolated thylakoid membranes

Fig. 2 shows the dependence on time of the photoinhibition at 5°C, 15°C and 25°C of oxygen evolution by thylakoid membranes from spinach and squash. The extent of photoinhibition was identical in the thylakoid

Table 1. IR frequency and absorbance obtained with transmission and reflection techniques with OHNS and DHCA LB films.

$\nu$ cm <sup>-1</sup>	Assignment	A <sub>T</sub>	A <sub>R</sub>	
2918	$\nu_{as}(\text{CH}_2)$	0.0091	0.0316	DHCA
		0.0072	0.0017	OHNS
2848	$\nu_s(\text{CH}_2)$	0.0059	0.0129	DHCA
		0.0036	0.001	OHNS
2213	$\nu(\text{C}_{AR}-\text{N})$	0.0021	0.0027	DHCA
1375	$\nu(\text{CN})$	0.0008	0.0021	DHCA
1509	$\nu(\text{C}_{AR}-\text{N})$	0.0036	0.001	OHNS
1336	$\nu_s(\text{NO}_2)$	0.0037	0.00039	OHNS
1249	$\nu(-\text{O}-)$	0.0021	0.00036	OHNS

$\nu$ : stretching vibration mode,  $\nu_{as}$ : asymmetric stretching mode,  $\nu_s$ : symmetric stretching mode

Arachidic acid was miscible with DHCA. We could not find any separated domain for arachidic acid and DHCA. The surface pressure-area isotherm of DHCA and arachidic acid mixture also showed no indication of phase separation. We found only limited number of highly contrasted small grain. No transitions in surface pressure-area isotherm of DHCA are consistent with low number of small grains.

The UV-visible absorption spectra of OHNS and DHCA LB films show J-aggregation peaks at 400 nm and 330 nm, respectively. Fig. 4 shows that the aggregation peak is larger than the monomer peak, and 420 nm peak indicates that extensive aggregation of OHNS occurred in the LB film. The thickness of OHNS and DHCA LB films measured is 150 Å and 23 Å, respectively. The thickness of LB films cannot be directly related to the morphology of Langmuir film. However, no polarization effects of Langmuir film and thickness of OHNS LB film can be explained by the double or quadruple layer at the air-water interface. The double and quadruple layers generate random orientation of chromophore moiety, due to the relaxation of chromophore orientation during the film transfer. The dichroic ratio of OHNS chromophore in LB was to be 1, which means random orientation in X-Y plane. The dichroic ratio of DHCA was found to be 0.78, and the rotation of analyzer of BAM produces image slight image inversion at the air-water interface.

A molecular orientation angle can be calculated from the reflection and transmission spectra. Characteristic IR vibration peaks of OHNS and DHCA were shown in Table 1. With the dichroic ratios of the transmission and the reflection absorbance, the orientation angle,  $\phi$ , of functional group of the molecules can be calculated with following Eq.<sup>12</sup>

$$\frac{A_T}{A_R} = \frac{\tan^2 \phi}{2m_z}$$

where A<sub>T</sub> is transmission absorbance, A<sub>R</sub> is reflection absorbance and  $m_z$  is intensity enhancement factors. The enhancement factors arise due to the metal surface use in RA measurement, and depend on five parameters: the frequency of the absorption band, the angle of incidence, the film thickness and the refractive index of film and substrate. The tilt angle of stilbene moiety of OHNS was calculated to be 45°, and cyanoaniline moiety of DHCA was 62° from surface normal.

The molecular orientation obtained with FT-IR spectroscopy can not apply directly to the molecular stacking for the OHNS films at the air-water interface. However the dichroic ratios of the film layered onto the solid substrate and little contrast change of the films at the air-water interface consistently support the disorder in X-Y plane. These may result from the random orientation of small domains and spots in X-Y plane. However the molecules with respect to the z axis retain their orientation. Both moderately polar aromatic molecules formed J-aggregates, which might collectively form small domains that can be observed with BAM.

*Acknowledgements* – This work was supported by KOSEF (grant #: 951-0301-038-2) and partially supported by KBSC.

## REFERENCES

1. Tsao, M-W., T. M. Fischer and C. M. Knobler (1995) Quantitative analysis of brewster-angle microscope images of tilt order in Langmuir monolayer domains, *Langmuir*, **11**, 3184-88.
2. Overbeck G. A. and D. Mobius (1993) A new phase in the generalized phase diagram of monolayer films of long-chain Fatty acids *J. Phys. Chem.* **97**, 7999-8004.
3. Overbeck, G. A., D. Honig and D. Mobius (1993) Visualization of first- and second-order phase transitions in eicosanol monolayers using brewster angle microscopy, *Langmuir*, **9**, 555-560.
4. Litvin, A., L. A. Samuelson, D. H. Charych, W. Specvak and D. Kaplan (1995) Liquid crystalline texture in glycine-modified diacetylene Langmuir monolayers at room temperature, *J. Phys. Chem.* **99**, 492-495.
5. Riviere, S., S. Heron, J. Meunier, D. K. Schwartz, M-W. Tsao and C. M. Knobler (1994) Texture and phase transitions in Langmuir monolayers of fatty acid. A comparative brewster angle microscope and polarized fluorescence microscope study, *J. Phys. Chem.* **101**, 10045-51.
6. Gehlert, U., G. Weidemann and D. Vollhardt (1995) Morphological features in 1-monoglyceride monolayers, *J. Coll. and Interface Sci.* **174**, 392-399.
7. Schwartz, D. K. M-W. Tsao and C. M. Knobler, (1994) Domain morphology in a two-dimensional anisotropy mesophase: cusps and boojum textures in a Langmuir monolayer, *J. Chem. Phys.* **101**, 8258-8261.
8. Hoover, J. M., M. D. Seltzer, J. D. Stemger-Smith, A. P.

- Chafin, R. A. Hollins and R. A. Henry (1994) *Polymer Preprints*, **35**, 266-7.
9. Shin, D. M. and O. Kwon (1994) Molecular orientation of intermolecular charge transfer aromatic molecules in the organized media, *J. Photoscience*, **1**, 53-59.
10. Shin, D. M., and O. Kwon (1995) Solvatochromic effects and hydrogen bonding interactions of 4-(4-Nitrophenylazo)-1-naphthol derivatives, *Bull. Korean Chem. Soc.*, **16**, 574-577.
11. Myers, D. (1991) Interfaces and Colloids, In *Surfaces*, pp. 248. VCH, Weinheim.
12. Umemura, J., T. Kamata, T. Kawai and T. Takenaka (1990) Quantitative evaluation of molecular orientation in thin Langmuir-Blodgett films by FT-IR transmission and reflection-absorption spectroscopy, *J. Phys. Chem.*, **94**, 62.